Bioconjugate Chemistry

Article

pubs.acs.org/bc

Neutral Polymeric Micelles for RNA Delivery

Brittany B. Lundy, Anthony Convertine, Martina Miteva, and Patrick S. Stayton*

Department of Bioengineering, University of Washington, Seattle, Washington 98195, United States

Supporting Information

ABSTRACT: RNA interference (RNAi) drugs have significant therapeutic potential, but delivery systems with appropriate efficacy and toxicity profiles are still needed. Here, we describe a neutral, ampholytic polymeric delivery system based on conjugatable diblock polymer micelles. The diblock copolymer contains a hydrophilic poly[*N*-(2-hydroxypropyl)methacrylamide-*co*-*N*-(2-(pyridin-2-yldisulfanyl)ethyl)methacrylamide) (poly[HPMA-*co*-PDSMA]) segment to promote aqueous stability and facilitate thiol−disulfide exchange reactions and a second ampholytic block composed of propylacrylic acid (PAA), dimethylaminoethyl methacrylate (DMAEMA), and butyl methacrylate (BMA). The poly[(HPMA-*co*-PDSMA)-*b*-(PAA-*co*-DMAEMA-*co*-BMA)] was synthesized using reversible addition−fragmentation chain transfer (RAFT) polymerization with an overall molecular weight of 22 000 g/mol and a PDI of 1.88. Dynamic light scattering and fluorescence measurements indicated that the diblock copolymers self-assemble under aqueous conditions to form polymeric micelles with a hydrodynamic radius and critical micelle concentration of 25 nm and 25 μg/mL, respectively. Red blood cell hemolysis experiments show that the neutral hydrophilic micelles have potent membrane destabilizing activity at endosomal pH values. Thiolated siRNA targeting glyceraldehyde 3-phosphate dehydrogenase (GAPDH) was directly conjugated to the polymeric micelles via thiol exchange reactions with the pyridal disulfide groups present in the micelle corona. Maximum silencing activity in HeLa cells was observed at a 1:10 molar ratio of siRNA to polymer following a 48 h incubation period. Under these conditions 90% mRNA knockdown and 65% protein knockdown at 48 h was achieved with negligible toxicity. In contrast the polymeric micelles lacking a pH-responsive endosomalytic segment demonstrated negligible mRNA and protein knockdown under these conditions. The potent mRNA knockdown and excellent biocompatibility of the neutral siRNA conjugates demonstrate the potential utility of this carrier design for delivering therapeutic siRNA drugs.

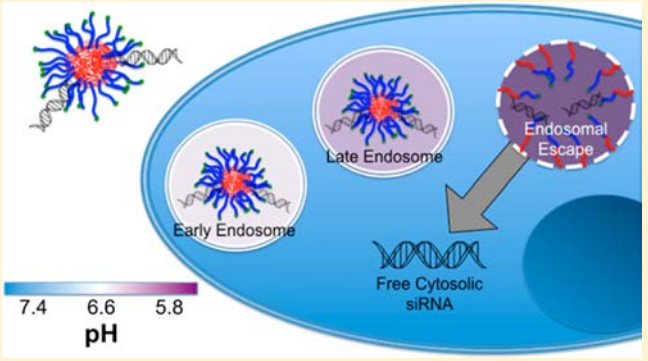

INTRODUCTION

Short interfering RNA (siRNA) technology has the potential to revolutionize the treatment of serious diseases by allowing selective silencing of oncogenic or therapeutic mRNAs and their corresponding proteins. Despite this immense therapeutic potential of this technology, the effective systemic and intracellular delivery of siRNA remains a significant challenge. The delivery of siRNA typically yields low levels of mRNA silencing due to barriers that include degradation by endo- and exonucleases, poor cellular uptake, and intracellular trafficking.[1]

To overcome these obstacles, delivery systems including liposomes, cationic lipoplexes, and cationic polymers have been developed to enhance the effectiveness of siRNA.[1−3] Because of their small size (∼100 nm), biocompatibility, and activity, liposomes have been used to successfully knock down the expression of proteins associated with a variety of disease targets.[4−9] Both cationic and neutral lipoplexes have exhibited good efficacy,[10−15] with different toxicity and protein adsorption/targeting properties that affect the choice of target tissue and medical application.[16,17] Cationic polymers, such as chitosan[18−21] and other natural polymers,[19,22] polyethylenimine (PEI),[23] dendrimers,[24,25] and other synthetic polymers[26,27] have also shown promise, although the toxicity of polycation carriers remains problematic.

Conjugation strategies have also been developed with a variety of nonviral delivery carrier systems. Lipophilic siRNA conjugates to cholesterol,[28] bile acids,[29,30] lipids,[31] and α-tocopherol (vitamin E)[32] have been shown to moderately increase target cell uptake. Cell-penetrating peptides such as TAT trans-activator protein,[33,34] Penetratin,[34,35] and Transportan[35] have also been conjugated to the antisense strand of siRNA to increase cellular uptake and enhance gene silencing. PEG−siRNA conjugates exhibit high levels of serum stability and have been shown to increase gene silencing efficiency.[36] Additionally, PEG−siRNA conjugates complexed with cationic polymers or peptides to form polyelectroplyte complex micelles, further enhancing circulation time, uptake, and efficacy.[37−40] Recently, Heredia et al. employed reversible addition−fragmentation chain transfer (RAFT) to prepare poly(ethylene glycol acrylate) with telechelic pyridyl disulfide

Received: August 30, 2012
Revised: January 24, 2013
Published: January 29, 2013

functionality.[41] Covalent siRNA conjugates have also been prepared by Xu et al. who conjugated siRNA to a pyridyl disulfide end-capped poly(HPMA)-dendritic carbohydrate scaffold.[42]

Previously, we described the synthesis of a new family of diblock copolymer siRNA carriers.[43−46] These carriers are composed of a positively charged block of dimethylaminoethyl methacrylate (DMAEMA) to mediate siRNA binding and a second pH-responsive endosomal-releasing block composed of DMAEMA, propylacrylic acid (PAA), and butyl methacylate (BMA) monomers. This carrier system displays excellent delivery activity, but the cationic segment could have adverse toxicity profiles. Here, we describe the development of a neutral, ampholytic diblock copolymer that replaces the cationic DMAEMA segment with a hydrophilic block of *N*-(2-hydroxypropyl)methacrylamide (HPMA) and a disulfide-conjugatable monomer *N*-(2-(pyridin-2-yldisulfanyl)ethyl)-methacrylamide. This system provides a starting foundation for future targeted siRNA delivery schemes using pH-responsive polymeric micelle conjugates for therapeutic use.

EXPERIMENTAL PROCEDURE

Materials. All reagents were purchased from Sigma-Aldrich and Wako Chemicals and used without further purification unless specified otherwise. The trithiocarbonate CTAs ethyl cyanovaleric trithiocarbonate (ECT) and PEG3 biotin ECT were synthesized as previously described.[43,47] Pyridyl disulfide methacrylate (PDSMA) was synthesized as described previously.[48] *N*,*N*-Dimethylacrylamide was distilled under reduced pressure. Propylacrylic acid (PAA) was synthesized as previously reported. Radical initiator (V70) was purchased from Wako Chemicals. 2,2-Azobisisobutyronitrile (AIBN) was recrystallized from methanol.

Synthesis of Poly(*N*-(2-hydroxypropyl)-methacrylamide (HPMA)-*co*-PDSMA) Macro Chain Transfer Agent (macroCTA). Poly(HPMA-*co*-PDSMA) was synthesized using a mixed aqueous−organic solvent system. Polymerizations were conducted with an initial molar HPMA to PDSMA ratio of 9:1. HPMA (1.134 g, 7.9 mmol) was dissolved in ultrapure water (5.87 g). Biotinylated 4-cyano-4-(ethylsulfanylthiocarbonyl)sulfanylvpentanoic acid (biotin-ECT) (93.8 mg, 0.106 mmol) was dissolved in ethanol (1 g). The initiator solution was prepared by dissolving V501 (1.23 mg/g ethanol solution, 4.38 μmol) in ethanol. PDSMA (0.225 g, 0.89 mmol) was dissolved in ethanol (1 g). The ethanol solutions were combined and added to the aqueous HPMA solution in a 25 mL round-bottom flask. The final solvent concentration was a ratio of 2:1 (water to ethanol). The solution was purged with nitrogen for 30 min on ice and then allowed to react at 70 °C for 4 h. Ultrapure water (35 g) was added to the reaction solution and frozen under liquid nitrogen. Water was removed from the reaction via lyphilization after 48 h. The resultant polymer was isolated by repeated precipitation from ethanol into an excess of ether. The polymer was rinsed after final precipitation with pentane to remove excess ether and dried overnight in a vacuum oven. The macroCTA was characterized by SEC to be 9300 g/mol with a PDI of 1.07 from the measured d*n*/d*c* of 0.091. ^{1}H NMR was used to determine the composition of 94% HPMA and 6% PDSMA by evaluating the peak at 3.9 ppm and aromatic peaks at resonances between 7 and 8.5 ppm for HPMA and PDSMA, respectively.

Synthesis of Poly[(HPMA-*co*-PDSMA)-*b*-(BMA-*co*-DMAEMA-*co*-PAA)]. Poly[(HPMA-*co*-PDSMA)-*b*-(BMA-*co*-DMAEMA-*co*-PAA)] was prepared by adding the poly-(HPMA-*co*-PDSMA) macroCTA (0.239 g, 28.5 μmol) to a solution of BMA (0.486 g, 3.42 mmol), DMAEMA (0.403 g, 2.56 mmol), and PAA (0.292 g, 2.56 mmol) (40:30:30 mol %) in dimethylacetamide (DMAc) (2.4 g) such that the final solvent concentration was 66% by weight. The initial macroCTA to V70 initiator (3.5 mg, 11.4 μmol) ratio ($[\text{macroCTA}]_o/[I]_o$) and initial monomer to macroCTA ($[M]_o/[\text{macroCTA}]_o$) were 2.5:1 and 300:1, respectively. The polymerization solution was purged with nitrogen for 30 min before being allowed to react at 30 °C for 24 h. The final polymers were isolated by precipitation from ethanol into a 50× excess of pentane/ether (3:1 v/v). The polymer precipitant was rinsed with neat pentane and dried under vacuum overnight. The polymers were dissolved in deionized water and further purified by passing them through PD10 desalting columns. The final dry polymers were obtained via lyophilization. The diblock copolymer was characterized by SEC to be 22 000 g/mol with a PDI of 1.88 from the measured d*n*/d*c* of 0.081. ^{1}H NMR was used to determine the composition of the second block to be 27% PAA, 24% DMAEMA, and 49% BMA, by evaluating the peaks between 3.9 and 4.2 ppm (representing HPMA, BMA, and DMAEMA), peak at 2.4 ppm (resonance peak of DAEMA), and the backbone peaks. The proportion of PAA was back-calculated from integrating the entire backbone peak and subtracting the protons associated with the other protons from HPMA, PDSMA, DMAEMA, and BMA.

Synthesis of Poly[(HPMA-*co*-PDSMA)-*b*-(methyl methacrylate) (MAA)] Non-pH-Responsive Control Polymer. The control polymer was prepared by adding the poly(HPMA-*co*-PDSMA) macroCTA (0.066 g, 7.92 μmol) to a solution of MAA (0.278 g, 2.77 mmol) in dimethylformamide (DMF) (0.416 g) such that the final solvent concentration was 55% by weight. The initial macroCTA to AIBN initiator (0.125 mg) ratio ($[\text{macroCTA}]_o/[I]_o$) and initial monomer to macroCTA ($[M]_o/[\text{macroCTA}]_o$) were 10:1 and 350:1, respectively. The polymerization solution was purged with nitrogen for 30 min before being allowed to react at 30 °C for 6 h. The final polymers were isolated by precipitation from DMF into a 50× excess of ether. The polymer precipitant was rinsed with neat ether and dried under vacuum overnight. The polymers were dissolved in deionized water and further purified by passing them through PD10 desalting columns. The final dry polymers were obtained via lyophilization. The diblock copolymer was characterized by SEC to be 17 300 g/mol with a PDI of 1.04 from the measure d*n*/d*c* of 0.0963.

Polymer Characterization. Absolute molecular weights and polydispersities (PDIs) were determined via SEC laser light scattering (LLS) using a Optimlab T-rEX (Wyatt) equipped with miniDAWN TREOS (Wyatt) for light scattering, refractive index, and UV. HPLC-grade DMF containing 0.1 wt % LiBr at 60 °C was used as the mobile phase at a flow rate of 1 mL/min. Copolymer composition was determined via ^{1}H NMR spectra, which were recorded on a Bruker AV301 in deuterated methanol (CD_3OD) at 25 °C. A deuterium lock (CD_3OD) was used, and chemical shifts were determined in ppm at 3.35 and 4.78 (CD_3OD). Polymer concentration was 7.5 mg/mL. Copolymer morphology was determined via ^{1}H NMR spectra and was recorded on a Bruker AV500 in CD_3OD

dx.doi.org/10.1021/bc300486k | *Bioconjugate Chem.* 2013, 24, 398−407

and deuterated oxide (D_2O) at 25 °C. Polymer concentration was 12.5 mg/mL.

Critical Micelle Concentration (cmc) via ANS Fluorescence. The cmc for the diblock copolymer was determined using a fluorescent probe, 1-anilino-8-naphthalene sulfonate (ANS). The ANS was dissolved in ethanol to form a 100 μM stock solution. Polymer concentration was varied from 1 to 100 μg/mL with a set ANS concentration of 5 μM. The various polymer solution (95 μL) was incubated with ANS stock solution (5 μL) for 1 h in a black 96-well Nunc plate. The fluorescence spectra (excitation, 390 nm; emission, 550 nm) were recorded using a Tecan Safire 2 microplate reader. The cmc was estimated to be the concentration corresponding to the half-width intensity at 550 nm between low and high plateau regions.

Transmission Electron Microscopy (TEM). A 1.0 mg/mL solution of poly[(HPMA-*co*-PDSMA)-*b*-(BMA-*co*-DMAEMA-*co*-PAA)] in PBS was applied to a carbon-coated copper grid for 30 min, fixed in Karnovsky's solution, and washed in cacodylate buffer and water. The grid was stained with a 6% solution of uranyl acetate for 15 min and then dried until analysis. Transmission electron microscopy was carried out on a Tecnai G2 F20, 200 kV scanning transmission electron microscope (S/TEM).

Dynamic Light Scattering. Particle sizes of polymer alone or polymer−siRNA conjugates were measured by dynamic light scattering (DLS) using a Malvern Zetasizer Nano ZS. Lyophilized polymer was dissolved in 100% ethanol at 10−50 mg/mL, then diluted 10-fold into phosphate buffer, pH 7.4. Polymers were analyzed in phosphate buffered saline, pH 7.4 (PBS), at 0.1 mg/mL for polymer alone and polymer−siRNA conjugates. Polymers and polymer−siRNA conjugates were filtered with a 200 nm filter prior to measurement.

siRNA Conjugation via Thiol Exchange. The number of thiol reactive pyridyl disulfide groups on the diblock copolymer was determined by following the release of pyridine-2-thione at 343 nm following a 60 min incubation period in pH 7.4 phosphate buffered saline (PBS) (137 mM NaCl, 2.7 mM KCl, 8 mM Na_2HPO_4, and 2 mM KH_2PO_4). The thiolated siRNA was reduced (GAPDH and SCR sequences) by combining 20 μL of thiolated siRNA stock solution (500 μM) with 45 μL of RNase-DNase free water and 50 μL of DTT (0.1 M) with 3 μL of triethylamine (TEA) (all values are per number of reactions).[42] Mixtures were incubated for 30 min, and the thiolated siRNA was isolated by precipitation into water saturated with ethyl acetate. The lyophilized diblock polymer was predissolved in 100% ethanol and then diluted 10-fold into phosphate buffer (RNase-DNase free), pH 7.4, at a final concentration of 2.5 mg/mL. Varying molar ratios of reactive PDS groups on polymer determined via TCEP reduction (1, 2, 5, 10, 20) were immediately added to siRNA solution (10 nmol of siRNA). Sterile phosphate buffer (RNase-DNase free), pH 7.4, was added to the final reaction have siRNA concentration of 11 μM and reacted at 37 °C for 12 h. The degree of siRNA conjugation to the block copolymer was determined by measuring the release of pyridine-2-thione at 343 nm using an extinction coefficient of 8.08×10^3 M^{-1} cm^{-1}.

Gel Shift Assay. To determine the polymer to thiol ratio at which complete siRNA conjugation occurs, gel retardation assays were conducted at varying molar ratios of polymeric PDS groups to thiolated siRNA. Ratios of 1:1, 2:1, 5:1, 10:1, and 20:1 (polymer reactive PDS groups to siRNA) were evaluated. A 2% agarose gel was loaded with each lane containing 1 μg of free siRNA or siRNA conjugated with varying quantities of diblock copolymer. An amount of 2 μL of a 0.1 M DTT solution was reacted with the conjugates for 1 h prior to loading on gel to evaluate the reversibility of the siRNA conjugation. An amount of 5 μL of 2.5% SDS solution was combined to siRNA conjugates to determine if electrostatic interactions were driving complexation rather than conjugation. Nonthiolated siRNA and the same polymer to siRNA ratios were also evaluated as controls. The gels were run at 100 V for 1 h and then stained with SYBR Safe dye diluted 1:5000 for 30 min for UV visualization.

Red Blood Cell Hemolysis Assay. pH responsive membrane destabilizing activity was assayed by titrating polymer alone or polymer−siRNA conjugates into preparations of human red blood cells (RBCs) and determining membranelytic activity by hemoglobin release (determined by measuring absorbance at 540 nm) under five different pH conditions. RBCs were isolated by centrifugation from whole blood collected in vaccutainers containing EDTA. RBCs were washed 3 times in normal saline and brought to a final concentration of 2% RBCs in PBS at a specific pH (5.8, 6.2, 6.6, 7.0, or 7.4). Polymer alone or polymer−siRNA conjugates were evaluated at 20 and 40 μg in triplicate at each pH. RBCs with polymer alone or polymer−siRNA conjugates were incubated at 37 °C for 60 min and centrifuged to remove intact RBCs. Supernatants were transferred to a transparent 96-well plate, and absorbance was determined at 540 nm. Percent hemolysis is expressed as A540 sample/A540 of 1% Triton X-100 treated RBCs (control for 100% lysis).

Cytotoxicity Measurements. Free diblock copolymer toxicity was evaluated in HeLa cells using the CellTiter 96AQueous One solution cell proliferation assay (MTS) (Promega Corp., Madison, WI). HeLa cells were seeded in 96-well plates at a density of 3000 cells/cm^2 and allowed to adhere overnight. The medium was then replaced with 200 μL of fresh medium containing the diblock copolymer at the appropriate concentrations. Polymer cytotoxicity was evaluated in triplicate after 12 h using the CellTiter MTS assay according to the manufacturer's instructions. The absorbance at 490 nm was evaluated using Tecan Safire 2 microplate reader, and untreated cells in the medium were used as a negative control.

The cytotoxicity of diblock copolymer and siRNA−polymer conjugates for normalization in the GAPDH protein assay was determined by assaying for cell metabolic activity. HeLa cells were seeded in 96-well plates at a density of 3000 cells/cm^2 and allowed to adhere overnight. Conjugates were formed with GAPDH siRNA at concentrations up to 100 nM siRNA/well (200 μL volume). Samples were added to wells in triplicate. After cells had been incubated for 24 or 48 h with the polymer or polymer−siRNA conjugates, the cells were lysed with KDalert lysis buffer and incubated at 4 °C for 20 min. An amount of 40 μL of cell lysate from each sample was then transferred to a fresh transparent 96-well plate and diluted with 60 μL of PBS buffer (pH 7.4). An amount of 100 μL of lactate dehydrogenase (LDH) reagent mix was then added to each well (Roche). The coupled enzymatic reaction occurred within 5 min at 25 °C, and fluorescence (490/650 nm) was determined according to the manufacturer's instructions. Percent viability is expressed as a function of 1% Triton X-100 treated cells (control for 0% viability).

Measurement of siRNA Knockdown Activity Using Quantitative PCR. Knockdown activity of siRNA−poly-[(HPMA-*co*-PDSMA)-*b*-(BMA-*co*-DMAEMA-*co*-PAA)] com-

plexes was assayed in 96-well format by measuring specific gene expression after 24 and 48 h of treatment with polymer−siRNA conjugates. Polymer and GAPDH targeting siRNA or negative control siRNA were mixed as described above and allowed to conjugate overnight before the addition to HeLa cells in 200 μL of normal medium containing 10% FBS. Final siRNA concentration was evaluated at 50 nM. Total RNA was isolated 24 and 48 h after treatment, and GAPDH expression was measured relative to the internal normalizer gene, B-actin, by quantitative PCR.

Measurement of siRNA Knockdown Activity by Measuring GAPDH Protein. HeLa cells were seeded in 96-well plates at a density of 3000 cells/cm^2 and allowed to adhere overnight. Conjugates were formed with GAPDH siRNA or negative control siRNA to attain concentrations up to 50 nM siRNA (200 μL volume). Ratios of 1:1, 2:1, 5:1, 10:1, and 20:1 (polymer PDS groups to siRNA) were evaluated. Samples were added to wells in triplicate. After cells had been incubated for 24 or 48 h with the polymer or polymer−siRNA conjugates, the cells were lysed and incubated at 4 °C for 20 min. The KDalert GAPDH assay kit (Ambion) was used to determine GAPDH protein levels. An amount of 10 μL of cell lysate from each sample was then transferred to a fresh black 96-well plate, and 90 μL of KDalert master mix was then added to each well. Fluorescence levels for each well were then read immediately after addition of the master mix (λ_{ex} = 560 nm and λ_{em} = 590 nm). Identical measurements were then repeated after 4 min. GAPDH activity was determined by the difference of the two readings. Values were then normalized to total lactate dehydrogenase (LDH) protein content via lysate analysis with LDH cytotoxicity kit (Roche) as previously described.

Polymer siRNA Conjugate Internalization by Fluorescence Microscopy. Internalization of diblock siRNA conjugates was visualized by fluorescence live-cell microscopy. HeLa cells were seeded in 96-well plates at a density of 15 000 cells/cm^2 and allowed to adhere overnight in Lab-Tek II chambered coverglass slides (NUNC, Rochester, NY). Polymer and polymer−siRNA conjugates were bound to Alexa-488-label streptavidin (4:1 M polymer to streptavidin) through the biotin RAFT agent after a 1 h incubation. Cells were treated with a 30 min incubation of polymer, polymer−siRNA conjugate, or streptavidin alone to look at internalization of the carrier at 1 h. Then a 25 nM steptavidin dose was administered to all sample groups. Chamber slides were placed on a live-cell fluorescence microscope (Nikon Ti-E) equipped with an environmental control chamber at 37 °C. Cells were imaged with a mercury lamp and a 100× objective using the following filter sets for AF488 and DAPI. Z-sections of the cells (step size 0.4 μm) were acquired, and after image acquisition image stacks were deconvolved using the object-based measurement software Volocity (Perkin-Elmer) to focus fluorescence. To deconvolve image stacks, point spread functions were calculated for the green and blue channels and applied using 25 iterations to reach a near 100% confidence interval.

RESULTS

Polymer Synthesis and Characterization. RAFT polymerization methodology was employed in order to prepare the macro chain transfer agent (macroCTA) composed predominately of the hydrophilic HPMA with 10 mol % (feed) of a thiol-reactive PDSMA comonomer as shown in Scheme 1. Aqueous conditions were selected for the copolymerization of the methacrylamido-based comonomers, as they have been

Scheme 1. Synthetic Structure, Molecular Weight, and Chemical Composition of the Diblock Copolymer for siRNA Conjugations Employed in These Studies

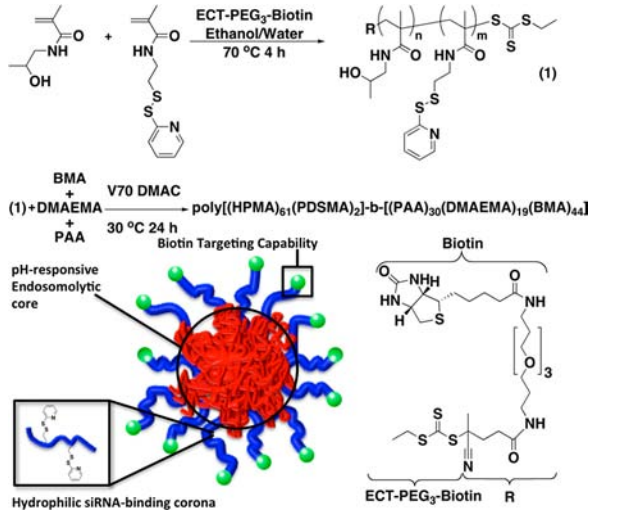

shown to provide excellent control over the molecular weight and polydispersity at lower initiator concentrations leading to materials high chain end retention of the thiocarbonylthio groups.[49,50] In order to facilitate solubilization of the poorly water-soluble PDSMA comonomer, 33% ethanol by volume was added to the aqueous polymerization solution. These conditions provided excellent control over the copolymerization as evidenced by the narrow and symmetric molecular weight distribution (Supporting Information Figure S1) and yielded a copolymer with a molecular weight and polydispersity of 9300 g/mol and 1.07, respectively. Incorporation of both comonomers in the copolymer as well as retention of PDS functionality was determined by ^{1}H NMR spectroscopy in CD_3OD. Comparison of the HPMA methyne resonance at 3.78 ppm to the PDSMA aromatic resonances at 8.45 ppm suggests that approximately 6% PDSMA was incorporated into the polymer compared to 10% in the feed (Table 1).

The resultant copolymer was subsequently employed as a macroCTA for block copolymerization of PAA, DMAEMA, and BMA. The polymerization was conducted in DMAc at 30 °C for 24 h. Although broadening of the molecular weight distribution was observed for the diblock copolymer, a clear shift to lower elution volumes is observed (Supporting Information Figure S1). Evaluation of the copolymer composition via ^{1}H NMR spectroscopy indicates approximately 49 mol % BMA content in the second block with approximately equimolar quantities of of PAA and DMAEMA making up the remainder (Figure 1). Also evident from the ^{1}H NMR spectrum is the presence of aromatic resonances associated with the PDS pyridine ring. Because the absolute concentration of PDSMA residues in the block copolymer is critically important for conjugation of thiolated siRNA, a TCEP reduction assay was also conducted to corroborate the values determined by ^{1}H NMR. In this assay the copolymer was dissolved in PBS buffer and incubated with 50 mM TCEP for 1 h in order to reduce disulfide bonds. It was determined that the number of PDS groups retained on the polymer was approximatey 1.9 compared to 2 PDS groups per polymer by NMR. A non-pH-reponsive control polymer containing a methyl methacrylate (MMA) based core (poly[(HPMA-*co*-PDSMA)-*b*-(MAA)]) was also synthesized via RAFT polymer-

dx.doi.org/10.1021/bc300486k | *Bioconjugate Chem.* 2013, 24, 398−407

Table 1. Molecular Weight and Chemical Composition of the Diblock Copolymer for siRNA Conjugations Employed in These Studies

polymer	composition (feed)	composition[a] (exp)	M_n [b] (g/mol)	PDI[b] (M_w/M_n)
($HPMA_{61}PDSMA_2$)	90:10	94:6	9300	1.07
($HPMA_{61}PDSMA_2$)-*b*-($PAA_{30}DMAEMA_{19}BMA_{44}$)	30:30:40	27:24:49	22000	1.88

[a]As determined by ^1H NMR (CD_3OD) spectroscopy (Bruker AV 500) (Figure 1). [b]As determined by size exclusion chromatography.

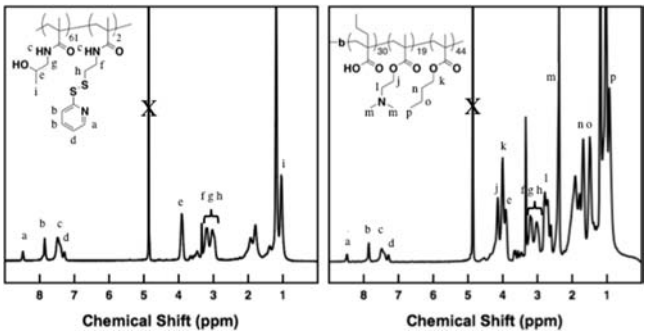

Figure 1. ^1H NMR spectra of the macroCTA and diblock copolymer in deuterated methanol (CD_3OD) at 25 °C: (a) is one proton from PDSMA, (e) is one proton from HPMA, (j) is two protons from DMAEMA, (k) is two protons from BMA, (m) is six protons from DMAEMA and the sum of protons from 0.5 to 3.1 ppm are from HPMA (10), DMAEMA (13), PDSMA (9), PAA (9), and BMA (12).

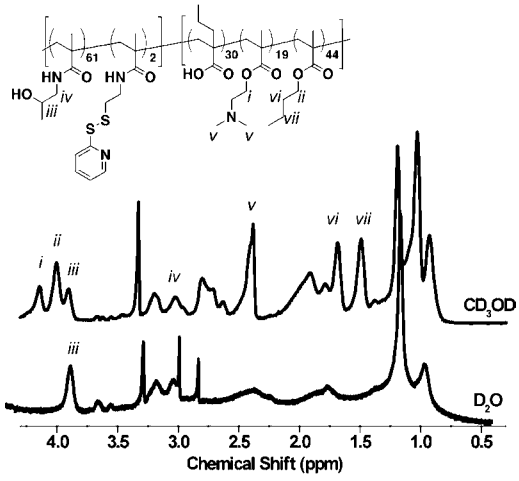

Figure 2. ^1H NMR spectra of the poly[(HPMA-*co*-PDSMA)-*b*-(PAA-*co*-DMAEMA-*co*-BMA)] in deuterated methanol (CD_3OD) and deuterated oxide (D_2O) at 25 °C represent polymer morphology based on environment. Resonances are associated with HPMA residues (iii, iv) as well as DMAEMA (i, v) and BMA (ii, vi, vii) fully solvated in CD_3OD, while a strong attenuation of resonances associated with DMAEMA (i, v) and BMA (ii) at 4.2, 2.4, and 4.0 ppm, respectively, is observed in D_2O.

ization and had an overall molecular weight of 17 300 g/mol with a PDI of 1.04.

Diblock Copolymer Morphology. Spectroscopic confirmation of the anticipated micellar morphology with a poly(HPMA-*co*-PDSMA) segment making up the corona and the poly(PAA-*co*-DMAEMA-*co*-BMA) segment making up the core was provided by ^1H NMR. Analysis of copolymer in deuterated methanol, which acts as a solvent for both block copolymer segments, shows resonances associated comonomer residues present in both blocks. This is clearly shown in Figure 2 where resonances associated with HPMA residues (iii, iv) as well as DMAEMA (i, v) and BMA (ii, vi, vii) are observed together. In contrast, NMR analysis of the diblock copolymer in D_2O shows a strong attenuation of resonances associated with the poly(PAA-*co*-DMAEMA-*co*-BMA) segment. This is illustrated in Figure 2 most notably by the disappearance ester resonances (DMAEMA and BMA; i, ii) at 4.2 and 4.0 ppm, respectively, as well as an almost complete disappearance of the strong DMAEMA dimethyl resonance (v) at 2.4 ppm. These results, taken together, strongly suggest the association of the diblock copolymers under aqueous conditions to form core shell particles. The peaks corresponding to the proton adjacent from the hydroxyl on HPMA (3.8 ppm) (iii) and the protons adjacent from the amide of HPMA (3.0 ppm) (iv) retain their intensity.

Self-assembly of the diblock copolymers into a micelle-like morphology under aqueous conditions was further supported by conducting dynamic light scattering measurements as a function of solution pH. Polymer and polymer siRNA conjugates were prepared in 1× PBS solutions (0.1 mg/mL) at pH 7.4, 6.6, and 5.8. Under physiological conditions, a hydrodynamic diameter from 25 to 27 nm was observed for polymer and siRNA−polymer conjugates (ratio of 20:1 PDS to siRNA); this is indicative of the expected micelle morphology. Under more acidic environments representative of the endocytosis pathway, a reduction in the hydrodynamic diameter was observed to below 10 nm, which is consistent with unimers and micelle disruption. This transition occurs when DMAEMA residues in the core-forming block become increasingly protonated, building up an excess cationic charge as PAA is protonated and becomes neutral. No significant size difference was observed with the addition of a reducing agent, TCEP, in solution under these conditions.

The critical micelle concentration (cmc) for the diblock copolymer was determined by following the change in fluorescence intensity of 8-anilino-1-naphthalenesulfonic acid (ANS) as a function of block copolymer concentration. ANS shows a significant increase in fluorescence intensity as well as a blue shift upon translocation from an aqueous solution to a nonpolar environment. By evaluation of the fluorescence intensity of ANS at 550 nm (370 nm excitation), it was possible to follow the transition of the diblock copolymer from an associated micellar state to unimers. Low ANS fluorescence is observed below a diblock copolymer concentration of approximately 10 μg/mL, while above this concentration a sharp increase in fluorescence occurs indicating a transition from unimers to micelles (Supporting Information Figure S2A). Measurements of the half-width intensity between low and high plateau regions indicate a cmc of ∼25 μg/mL for the diblock copolymer derived micelles. Additional evidence that the diblock copolymer exists in particle morphology was evaluated by electron microscopy (Supporting Information Figure S2B). From the electron micrograph the average diameters of the particles, which appear spherical, are sub-50 nm.

Polymer−siRNA Conjugation and Characterization by Gel Electrophoresis. To conjugate polymer and siRNA via

dx.doi.org/10.1021/bc300486k | *Bioconjugate Chem.* 2013, 24, 398−407

reducible disulfide linkages, thiolated siRNA molecules were first reduced with DTT for 30 min and then reacted with the PDS–functional diblock copolymer overnight at 37 °C. Polymer–siRNA conjugation efficiency was determined via agarose gel electrophoresis and by analysis of pyridine-2-thione release. Thiol to PDS ratios of 1:1, 1:2, and 1:10 (thiol to polymer, ∼1:0.5, 1:1, and 1:5) were evaluated in order to determine the minimum ratio necessary to achieve complete siRNA conjugation. This value was determined to be 1:10 (thiol to polymer, ∼1:5) as evidenced by gel electrophoresis where a complete disappearance of the free siRNA band is observed at this ratio (Supporting Information Figure S3). As expected, siRNA conjugations conducted at a thiol to PDS ratio of 1:20 also showed complete siRNA conjugation (Figure 3).

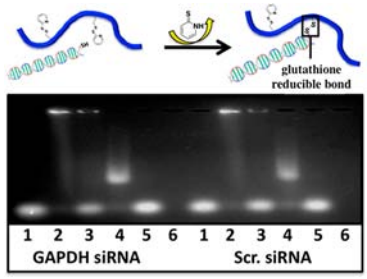

Figure 3. Gel retardation assay validating polymer–siRNA conjugation via a reducible disulfide bond, 1 μg siRNA/lane: free thiolated siRNA (lane 1), 20:1 (reactive PDS groups on polymer to thiolated siRNA) polymer–siRNA conjugate (lane 2); polymer–siRNA conjugate and 0.1 M DTT (lane 3); polymer–siRNA conjugate and 1% SDS (lane 4); polymer–siRNA conjugate, 0.1 M DTT, and 1% SDS (lane 5); free polymer (lane 6).

Following incubation with DTT, a disulfide reducing agent that cleaves the siRNA–polymer linkage, electrophoresis of the conjugates resulted in a reappearance of the free siRNA band. Following incubation with SDS, which disrupts micelle formulation, electrophoresis of the conjugates indicated no band corresponding to free siRNA, suggesting that the siRNA molecules remained conjugated to the unimer form of the polymer. Complete siRNA reduction from the polymeric system was observed under the presence of DTT and SDS perhaps because the DTT was allowed access to the bond without steric hindrance from the micelle formation. Control experiments in which nonthiolated siRNA was incubated in the presence of the diblock copolymer did not result in any visible associations with the polymer. Comparison of thiolated GAPDH siRNA to the corresponding scrambled sequence showed negligible differences in the pyridine-2-thione release, particle sizes, and conjugation reversibility assays. In addition, siRNA conjugation was successful at this ratio to the non-pH-responsive control polymer (data not shown).

pH-Responsive Membrane Destabilizing Activity. The pH-responsive membrane destabilizing activity of diblock copolymer was assayed using a red blood cell hemolysis assay. Five different pH conditions were used to mimic the transitions within the endosomal pH environments ranging from extracellular pH 7.4 to late endosome pH 5.8. Membrane destabilization is thought to occur through a combination of ionic localization of the polymer on the membrane surface and hydrophobic interaction of the nonpolar butyl methacrylate with the membrane lipids. To test whether conjugation of the diblock copolymer to a hydrophilic nucleic acid interfered with the intrinsic membrane disruptive properties of the polymer, hemolysis experiments were conducted on both the polymer alone and the polymer–siRNA conjugates for both the GAPDH and SCR siRNA sequences with a final polymer concentration at 40 μg/mL (Figure 4). No significant

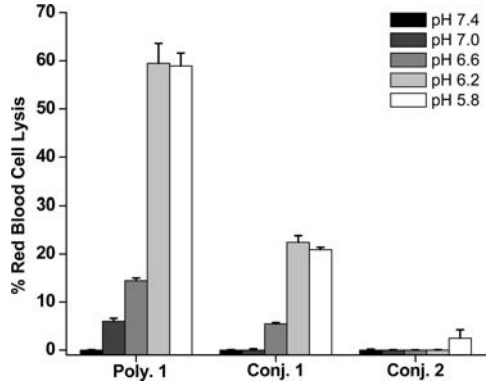

Figure 4. Hemolysis of the poly[(HPMA-*co*-PDSMA)-*b*-(PAA-*co*-DAEMA-*co*-BMA)] diblock copolymer, poly[(HPMA-*co*-PDSMA)-*b*-(PAA-*co*-DAEMA-*co*-BMA)] diblock copolymer–siRNA conjugates (Conj. 1), and poly[(HPMA-*co*-PDSMA)-*b*-(MMA)] diblock copolymer–siRNA conjugates (Conj. 2) both at a 20:1 of the reactive PDS groups on the polymer to thiolated siRNA at pH concentrations of 5.8, 6.2, 6.6, and 7.4 of 40 μg polymer/mL. Hemolytic activity is normalized relative to a positive control, 1% v/v Triton X-100, and the data represent a single experiment conducted in triplicate ± standard deviation.

hemolytic activity was observed at pH 7.4 for polymer and polymer–siRNA conjugates. Significant increases in red blood cell lysis were observed as pH was reduced to 6.2. Under these conditions, similar hemolytic properties were observed between the both GAPDH and SCR sequence siRNA–polymer conjugates. The maximum hemolytic activity was approximately one-third of the value for free polymer alone, suggesting that the RNA does attenuate the membrane-destabilizing activity when conjugated. Attenuation of the polymer intrinsic membrane disruptive properties, as shown by the red blood cell hemolysis assay, is generally proposed to be a result of altering the individual polymer chain's hydrophilic–hydrophobic balance. The pH-responsive segment becomes sharply membrane destabilizing as the propyl acrylic acid is protonated to neutrality, where the alkyl segment can destabilize membrane packing together with the butylmethacrylate alkyl segments. More specifically, there could also be activity reducing effects of ionic interactions between the negatively charge siRNA and the endosomolytic segment as the pH drop increases the net positive charge of this block. The non-pH-responsive control polymer and siRNA–polymer conjugates exhibited no hemolytic activity at all pH ranges.

Polymer–siRNA Conjugate Internalization. In order to evaluate the presence of polymer–siRNA conjugates within the HeLa cells, nanoparticles were incubated for 1 h at room temperature with an Alexa-488 labeled streptavidin (SA) to bind the biotin on the RAFT chain transfer agent. The SA–polymer–siRNA conjugates were then added to the cell medium at a dose of 25 nM. After a 30 min incubation with the SA–polymer–siRNA conjugates and a medium wash, cells demonstrated robust intracellular fluorescence, suggesting that internalization had occurred. Free SA alone was not visualized within the cells (Supporting Information Figure S4).

dx.doi.org/10.1021/bc300486k | *Bioconjugate Chem.* 2013, 24, 398–407

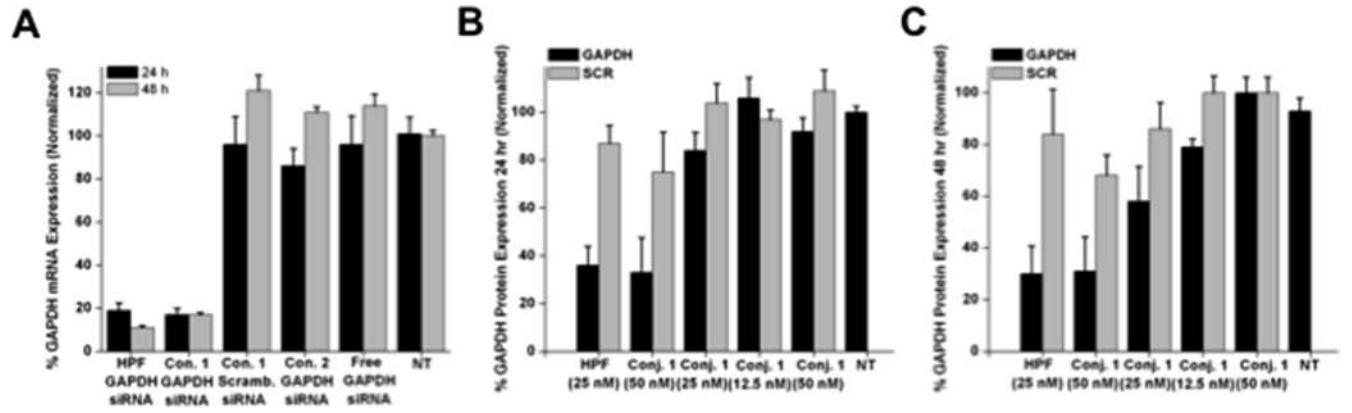

Figure 5. (A) GAPDH mRNA knockdown in HeLa cells was measured using real time RT-PCR following a 24 and 48 h incubation with the poly[(HPMA-*co*-PDSMA)-*b*-(PAA-*co*-DAEMA-*co*-BMA)] diblock copolymer−siRNA conjugates (Con. 1) and poly[(HPMA-*co*-PDSMA)-*b*-(MMA)] diblock copolymer−siRNA conjugates (Con. 2) both at a 20:1 of the reactive PDS groups on the polymer to thiolated siRNA at 50 nM doses. Scrambled siRNA conjugates and a commercially available transfection reagent, Hiperfect, were used as negative and positive controls, respectively. The data are represented with a $N = 6 \pm$ standard error. (B, C) GAPDH protein knockdown in HeLa cells was measured using KDalert GAPDH assay following 24 and 48 h incubation periods with poly[(HPMA-*co*-PDSMA)-*b*-(PAA-*co*-DAEMA-*co*-BMA)] diblock copolymer−siRNA conjugates (12.5, 25, and 50 nM siRNA dose). Data were normalized with an LDH toxicity assay. Scrambled siRNA conjugates and a commercially available transfection reagent, Hiperfect, were used as negative and positive controls, respectively. The data are represented with a $N = 6$, ±standard deviation.

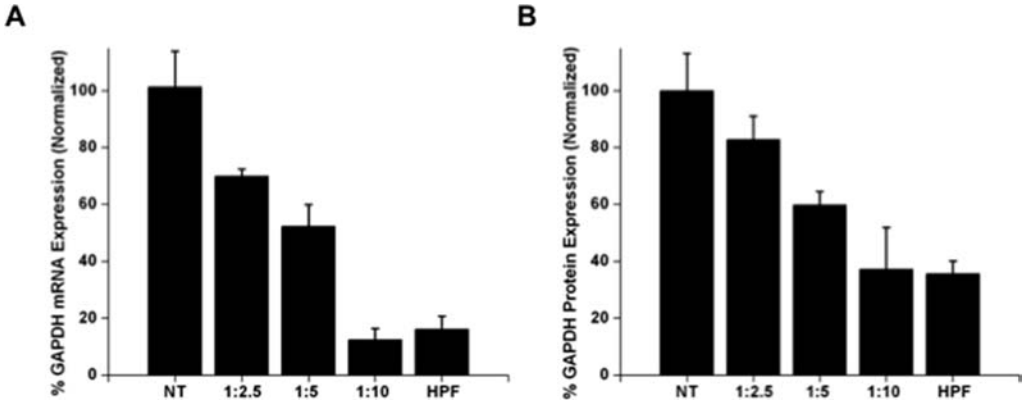

Figure 6. (A) GAPDH mRNA knockdown in HeLa cells was measured using real time RT-PCR following a 24 h incubation with the poly[(HPMA-*co*-PDSMA)-*b*-(PAA-*co*-DAEMA-*co*-BMA)] diblock copolymer−siRNA conjugates at a 1:2.5, 1:5, and 1:10 of the thiolated siRNA to the diblock copolymer at a 50 nM siRNA dose. A commercially available transfection reagent, Hiperfect, was used as a positive control. The data are represented with a $N = 6$, ±standard error. (B) GAPDH protein knockdown in HeLa cells was measured using KDalert GAPDH assay following a 48 h incubation period with poly[(HPMA-*co*-PDSMA)-*b*-(PAA-*co*-DAEMA-*co*-BMA)] diblock copolymer−siRNA conjugates (50 nM GAPDH siRNA dose) with a range of siRNA to diblock copolymer ratios. Data were normalized with an LDH toxicity assay. A commercially available transfection reagent, Hiperfect, was used as a positive control. The data are represented with a $N = 6$, ±standard deviation.

siRNA Conjugates Are Active in Vitro. The knockdown activity of the pH-responsive siRNA−polymer conjugate was evaluated in HeLa cells. siRNA directed against GAPDH (or a scrambled negative control) was conjugated to the polymer carrier and added directly to HeLa cells in medium containing 10% FBS for a 48 h continuous incubation. The final siRNA concentration was evaluated at 50 nM for the polymer−siRNA conjugates and 25 nM for the commercially available siRNA delivery agent Hiperfect. The high intrinsic toxicity of Hiperfect limited the maximum siRNA dose for the control to 25 nM. Above this concentration a substantial loss in cell viability was observed. Specific gene knockdown activity was then measured 24 and 48 h after transfection via real-time quantitative PCR (Figure 5A). GAPDH−polymer conjugates successfully reduced GAPDH mRNA to 17% and 11% control at 24 and 48 h, respectively. Negative control SCR−polymer conjugates did not show any knockdown GAPDH mRNA activity at either time point. Cell toxicity was evaluated with an MTS assay, and it verified that the polymer and polymer−siRNA conjugates up to 3 orders of magnitude above reasonable siRNA doses are nontoxic in Helas cells (Supporting Information Figure S5).

The ability of the siRNA−polymeric conjugates to deliver active siRNA was further evaluated by assaying the amount of GAPDH protein in HeLa cells (Figure 5B). GAPDH protein knockdown activity was then measured 24 and 48 h after transfection via KDalert GAPDH assay kit. GAPDH−polymer conjugates successfully reduced GAPDH protein levels to 50% of controls at 24 h of incubation and 35% of controls at 48 h of incubation at 50 nM siRNA dose in HeLas. Negative control SCR−polymer conjugates failed to exhibit GAPDH protein knockdown. To evaluate the effect of the polymer on the ability to effect siRNA knockdown, various ratios of conjugated siRNA to polymer were tested at a fixed siRNA dose of 50 nM. A higher dose of polymer (lower siRNA to polymer ratio during

dx.doi.org/10.1021/bc300486k | *Bioconjugate Chem.* 2013, 24, 398−407

conjugation) in the siRNA–polymer conjugates resulted in a greater ability to knockdown GAPDH without increasing toxicity in this concentration range (Figure 6). Physical mixtures of nonthiolated siRNA and polymers showed negligible protein knockdown activity (Supporting Information Figure S6).

DISCUSSION

Delivery challenges still limit the therapeutic potential of siRNA.[51] Considerable progress has been made in siRNA drug development with liposomal carriers for liver applications.[52,53] These carriers can have excellent therapeutic indices due to both passive and intrinsic targeting to the liver. They can also be designed to enhance endosomal release via proton sponge and/or lipid phase effects directly on the endosomal membrane. While lipid-based systems have led the way in the siRNA delivery field, a critical need exists for better carriers that work in other disease target tissues and with good toxicity profiles. In this work have described an endosomal-releasing siRNA delivery system that retains delivery activity within a neutral, ampholytic diblock copolymer micelle system. The carrier exploits a reducible disulfide conjugation strategy for linking the siRNA to the micelle carrier. This approach allows for direct conjugation of thiolated siRNA drugs directly to the polymeric scaffold without the need for a polycation segment.

The cytotoxicity of our neutral corona nanocarrier is strikingly reduced compared to the polycation corona composition with negligible toxicity observed in HeLa cells even after 24 h of continuous exposure at 500 μg/mL polymer.[44] Successful disulfide formation between thiolated siRNA and the PDS functional polymer was quantitated via pyridine-2-thione release and agarose gel electrophoresis. These studies suggest that greater than 95% siRNA conjugation was observed at a siRNA to PDS ratio of 1:20. GAPDH–polymer conjugates at 50 nM doses successfully reduced GAPDH mRNA to 17% and 11% of the untreated control levels at 24 and 48 h, respectively. No reduction in GAPDH levels was observed for physical mixture of the diblock copolymer micelles with siRNA lacking thiol functionality. This finding supports the conclusion that reversible covalent association of the siRNA to the micelle is necessary to achieve cytoplasmic delivery. Control experiments conducted with micelle carriers containing an inert micelle core lacking any pH-responsive membrane destabilizing behavior (i.e., poly(methyl methacrylate)) also showed negligible mRNA knockdown. The strong correlation between the hemolytic activity of the siRNA conjugates and the ability to knock down the GAPDH protein indicate that an endosomal releasing core provides a significant intracellular delivery advantage in this carrier system.

CONCLUSIONS

Here, we have reported the development of a neutral, ampholytic polymer micelle carrier for siRNA delivery that exploits direct disulfide drug conjugation. By use of RAFT polymerization, a [(HPMA-*co*-PDSMA)-*b*-(DMAEMA-*co*-PAA-*co*-BMA)] diblock copolymer was synthesized with 2 mol % PDS groups per polymer chain. Thiolated siRNA was reacted with the pyridyl disulfide moieties incorporated into the hydrophilic block to achieve approximately one to two siRNA molecules per micelle with an average diameter of 25 nm. The siRNA conjugates retain the pH-responsive membrane-destabilizing activity of the parent polymer, although the absolute activity is attenuated by conjugation. The siRNA–polymer linkages are reducible by glutathione, and conjugation is required for the knockdown of GAPDH mRNA and protein. These carriers exhibit maximum mRNA and protein knockdown at 50 nM siRNA doses in HeLa cells with a siRNA linear dose–response curve. The effectiveness and low cytotoxicity of this new carrier make it a promising candidate for future in vivo siRNA delivery studies in disease models.

ASSOCIATED CONTENT

Supporting Information

Size exclusion chromatographs for p(HPMA-*co*-PDSMA), p[(HPMA-*co*-PDSMA)-*b*-(PAA-*co*-DMAEMA-*co*-BMA)], and p[(HPMA-*co*-PDSMA)-*b*-(MAA)]; cmc of diblock copolymer via ANS fluorescence; polymer–siRNA conjugation at various ratios via gel retardation assay; polymer–siRNA uptake via fluorescent microscopy; polymer toxicity via MTS assay in HeLa cells after 24 h of incubation; GAPDH protein knockdown with nonthiolated siRNA and polymer. This material is available free of charge via the Internet at http://pubs.acs.org.

AUTHOR INFORMATION

Corresponding Author

*Phone: (206) 685-8148. Fax: (206) 685-8526. E-mail: stayton@u.washington.edu.

Notes

The authors declare the following competing financial interest(s): Professor Stayton has a financial interest in the company PhaseRx Inc. that has licensed some of the drug delivery technology described in this work. However, this work was entirely conducted at the University of Washington without funding or scientific connections to PhaseRx Inc.

ACKNOWLEDGMENTS

We acknowledge Scott Braswell at University of Washington's NanoTech User Facility for his assistance with electron microscopy. This work was funded by the National Institutes of Health (Grant R01EB002991 and Grant 1R21EB014572-01A1), The Life Science Discovery Fund (Grant 2496490), and the National Science Foundation Graduate Fellowship.

ABBREVIATIONS

ANS, 1-anilino-8-naphthalene sulfonate; BMA, butyl methacrylate; CTA, chain transfer agent; DMAEMA, dimethylaminoethyl methacrylate; DTT, dithiothreitol; GAPDH, glyceraldehyde 3-phosphate dehydrogenase; HPMA, *N*-(2-hydroxypropyl)-methacrylamide; LDH, lactate dehydrogenase; MAA, methyl methacrylate; PAA, propylacrylic acid; PDS, pyridyl disulfide; PDSMA, pyridyl disulfide methacrylate; RAFT, reversible addition–fragmentation chain transfer; RNAi, RNA interference; SA, streptavidin; SCR, scrambled; SDS, sodium dodecyl sulfate; siRNA, short interfering RNA; TCEP, tris(2-carboxyethyl)phosphine

REFERENCES

(1) Shim, M. S., and Kwon, Y. J. (2010) Efficient and targeted delivery of siRNA in vivo. *FEBS J. 277*, 4814–4827.

(2) Aliabadi, H. M., Landry, B., Sun, C., Tang, T., and Uludağ, H. (2012) Supramolecular assemblies in functional siRNA delivery: Where do we stand? *Biomaterials 33*, 2546–2569.

(3) Whitehead, K. A., Langer, R., and Anderson, D. G. (2009) Knocking down barriers: advances in siRNA delivery. *Nat. Rev. Drug Discovery 8*, 129−138.
(4) Guo, P., Coban, O., Snead, N. M., Trebley, J., Hoeprich, S., Guo, S., and Shu, Y. (2010) Engineering RNA for targeted siRNA delivery and medical application. *Adv. Drug Delivery Rev. 62*, 650−666.
(5) Landen, C., Chavez-Reyes, A., Bucana, C., Schmandt, R., Deavers, M., Lopez-Berestein, G., and Sood, A. (2005) Therapeutic EphA2 gene targeting in vivo using neutral liposomal small interfering RNA delivery. *Cancer Res. 65*, 6910−6918.
(6) Tran, M. A., Watts, R. J., and Robertson, G. P. (2009) Use of liposomes as drug delivery vehicles for treatment of melanoma. *Pigm. Cell Melanoma Res. 22*, 388−399.
(7) Villares, G. J. G., Zigler, M. M., Wang, H. H., Melnikova, V. O. V., Wu, H. H., Friedman, R. R., Leslie, M. C. M., Vivas-Mejia, P. E. P., Lopez-Berestein, G. G., Sood, A. K. A., and Bar-Eli, M. M. (2008) Targeting melanoma growth and metastasis with systemic delivery of liposome-incorporated protease-activated receptor-1 small interfering RNA. *CORD Conf. Proc. 68*, 9078−9086.
(8) Halder, J. J., Kamat, A. A. A., Landen, C. N. C., Han, L. Y. L., Lutgendorf, S. K. S., Lin, Y. G. Y., Merritt, W. M. W., Jennings, N. B. N., Chavez-Reyes, A. A., Coleman, R. L. R., Gershenson, D. M. D., Schmandt, R. R., Cole, S. W. S., Lopez-Berestein, G. G., and Sood, A. K. A. (2006) Focal adhesion kinase targeting using in vivo short interfering RNA delivery in neutral liposomes for ovarian carcinoma therapy. *Clin. Cancer Res. 12*, 4916−4924.
(9) Sato, A., Takagi, M., Shimamoto, A., Kawakami, S., and Hashida, M. (2007) Small interfering RNA delivery to the liver by intravenous administration of galactosylated cationic liposomes in mice. *Biomaterials 28*, 1434−1442.
(10) Chien, P.-Y. P., Wang, J. J., Carbonaro, D. D., Lei, S. S., Miller, B. B., Sheikh, S. S., Ali, S. M. S., Ahmad, M. U. M., and Ahmad, I. I. (2005) Novel cationic cardiolipin analogue-based liposome for efficient DNA and small interfering RNA delivery in vitro and in vivo. *Cancer Gene Ther. 12*, 321−328.
(11) Pal, A. A., Ahmad, A. A., Khan, S. S., Sakabe, I. I., Zhang, C. C., Kasid, U. N. U., and Ahmad, I. I. (2005) Systemic delivery of RafsiRNA using cationic cardiolipin liposomes silences Raf-1 expression and inhibits tumor growth in xenograft model of human prostate cancer. *Int. J. Oncol. 26*, 1087−1091.
(12) Basha, G., Novobrantseva, T. I., Rosin, N., Tam, Y. Y. C., Hafez, I. M., Wong, M. K., Sugo, T., Ruda, V. M., Qin, J., Klebanov, B., Ciufolini, M., Akinc, A., Tam, Y. K., Hope, M. J., and Cullis, P. R. (2011) Influence of cationic lipid composition on gene silencing properties of lipid nanoparticle formulations of siRNA in antigen-presenting cells. *Mol. Ther. 19*, 2186−2200.
(13) Semple, S. C., Akinc, A., Chen, J., Sandhu, A. P., Mui, B. L., Cho, C. K., Sah, D. W. Y., Stebbing, D., Crosley, E. J., Yaworski, E., Hafez, I. M., Dorkin, J. R., Qin, J., Lam, K., Rajeev, K. G., Wong, K. F., Jeffs, L. B., Nechev, L., Eisenhardt, M. L., Jayaraman, M., Kazem, M., Maier, M. A., Srinivasulu, M., Weinstein, M. J., Chen, Q., Alvarez, R., Barros, S. A., De, S., Klimuk, S. K., Borland, T., Kosovrasti, V., Cantley, W. L., Tam, Y. K., Manoharan, M., Ciufolini, M. A., Tracy, M. A., de Fougerolles, A., MacLachlan, I., Cullis, P. R., Madden, T. D., and Hope, M. J. (2010) Rational design of cationic lipids for siRNA delivery. *Nat. Biotechnol. 28*, 172−176.
(14) Huang, Y.-H., Bao, Y., Peng, W., Goldberg, M., Love, K., Bumcrot, D. A., Cole, G., Langer, R., Anderson, D. G., and Sawicki, J. A. (2009) Claudin-3 gene silencing with siRNA suppresses ovarian tumor growth and metastasis. *Proc. Natl. Acad. Sci. U.S.A. 106*, 3426−3430.
(15) Leuschner, F. F., Dutta, P. P., Gorbatov, R. R., Novobrantseva, T. I. T., Donahoe, J. S. J., Courties, G. G., Lee, K. M. K., Kim, J. I. J., Markmann, J. F. J., Marinelli, B. B., Panizzi, P. P., Lee, W. W. W., Iwamoto, Y. Y., Milstein, S. S., Epstein-Barash, H. H., Cantley, W. W., Wong, J. J., Cortez-Retamozo, V. V., Newton, A. A., Love, K. K., Libby, P. P., Pittet, M. J. M., Swirski, F. K. F., Koteliansky, V. V., Langer, R. R., Weissleder, R. R., Anderson, D. G. D., and Nahrendorf, M. M. (2011) Therapeutic siRNA silencing in inflammatory monocytes in mice. *Nat. Biotechnol. 29*, 1005−1010.
(16) Hashida, M., Kawakami, S., and Yamashita, F. (2005) Lipid carrier systems for targeted drug and gene delivery. *Chem. Pharm. Bull. (Tokyo) 53*, 871−880.
(17) Mahon, K. P., Love, K. T., Whitehead, K. A., Qin, J., Akinc, A., Leshchiner, E., Leshchiner, I., Langer, R., and Anderson, D. G. (2010) Combinatorial approach to determine functional group effects on lipidoid-mediated siRNA delivery. *Bioconjugate Chem. 21*, 1448−1454.
(18) Howard, K. A., Rahbek, U. L., Liu, X., Damgaard, C. K., Glud, S. Z., Andersen, M. O., Hovgaard, M. B., Schmitz, A., Nyengaard, J. R., Besenbacher, F., and Kjems, J. (2006) RNA interference in vitro and in vivo using a chitosan/siRNA nanoparticle system. *Mol. Ther. 14*, 476−484.
(19) Howard, K. A., Paludan, S. R., Behlke, M. A., Besenbacher, F., Deleuran, B., and Kjems, J. (2009) Chitosan/siRNA nanoparticle-mediated TNF-alpha knockdown in peritoneal macrophages for anti-inflammatory treatment in a murine arthritis model. *CORD Conf. Proc. 17*, 162−168.
(20) Sarmento, B., and das Neves, J., Eds. (2012) *Chitosan-Based Systems for Biopharmaceuticals*, p 592, Wiley, Chichester, U.K.
(21) Pillé, J.-Y. J., Li, H. H., Blot, E. E., Bertrand, J.-R. J., Pritchard, L.-L. L., Opolon, P. P., Maksimenko, A. A., Lu, H. H., Vannier, J.-P. J., Soria, J. J., Malvy, C. C., and Soria, C. C. (2006) Intravenous delivery of anti-RhoA small interfering RNA loaded in nanoparticles of chitosan in mice: safety and efficacy in xenografted aggressive breast cancer. *Hum. Gene Ther. 17*, 1019−1026.
(22) Heidel, J. D., Yu, Z., Liu, J. Y.-C., Rele, S. M., Liang, Y., Zeidan, R. K., Kornbrust, D. J., and Davis, M. E. (2007) Administration in non-human primates of escalating intravenous doses of targeted nanoparticles containing ribonucleotide reductase subunit M2 siRNA. *Proc. Natl. Acad. Sci. U.S.A. 104*, 5715−5721.
(23) Wightman, L. L., Kircheis, R. R., Rössler, V. V., Carotta, S. S., Ruzicka, R. R., Kursa, M. M., and Wagner, E. E. (2001) Different behavior of branched and linear polyethylenimine for gene delivery in vitro and in vivo. *J. Gene Med. 3*, 362−372.
(24) Wang, Y., Li, Z., Han, Y., Liang, L. H., and Ji, A. (2010) Nanoparticle-based delivery system for application of siRNA in vivo. *Curr. Drug Metab. 11*, 182−196.
(25) Kim, I.-D., Lim, C.-M., Kim, J.-B., Nam, H. Y., Nam, K., Kim, S.-W., Park, J.-S., and Lee, J.-K. (2010) Neuroprotection by biodegradable PAMAM ester (e-PAM-R)-mediated HMGB1 siRNA delivery in primary cortical cultures and in the postischemic brain. *J. Controlled Release 142*, 422−430.
(26) Watanabe, K., Harada-Shiba, M., Suzuki, A., Gokuden, R., Kurihara, R., Sugao, Y., Mori, T., Katayama, Y., and Niidome, T. (2009) In vivo siRNA delivery with dendritic poly(L-lysine) for the treatment of hypercholesterolemia. *Mol. BioSyst. 5*, 1306−1310.
(27) Khan, A., Benboubetra, M., Sayyed, P. Z., Ng, K. W., Fox, S., Beck, G., Benter, I. F., and Akhtar, S. (2004) Sustained polymeric delivery of gene silencing antisense ODNs, siRNA, DNAzymes and ribozymes: in vitro and in vivo studies. *J. Drug Targeting 12*, 393−404.
(28) Soutschek, J., Akinc, A., Bramlage, B., Charisse, K., Constien, R., Donoghue, M., Elbashir, S., Geick, A., Hadwiger, P., Harborth, J., John, M., Kesavan, V., Lavine, G., Pandey, R. K., Racie, T., Rajeev, K. G., Röhl, I., Toudjarska, I., Wang, G., Wuschko, S., Bumcrot, D., Koteliansky, V., Limmer, S., Manoharan, M., and Vornlocher, H.-P. (2004) Therapeutic silencing of an endogenous gene by systemic administration of modified siRNAs. *Nature 432*, 173−178.
(29) Wolfrum, C., Shi, S., Jayaprakash, K. N., Jayaraman, M., Wang, G., Pandey, R. K., Rajeev, K. G., Nakayama, T., Charrise, K., Ndungo, E. M., Zimmermann, T., Koteliansky, V., Manoharan, M., and Stoffel, M. (2007) Mechanisms and optimization of in vivo delivery of lipophilic siRNAs. *Nature 25*, 1149−1157.
(30) Musacchio, T., Vaze, O., D'Souza, G., and Torchilin, V. P. (2010) Effective stabilization and delivery of siRNA: reversible siRNA-phospholipid conjugate in nanosized mixed polymeric micelles. *Bioconjugate Chem. 21*, 1530−1536.

(31) Lorenz, C., Hadwiger, P., John, M., Vornlocher, H. P., and Unverzagt, C. (2004) Steroid and lipid conjugates of siRNAs to enhance cellular uptake and gene silencing in liver cells. *Bioorg. Med. Chem. Lett. 14*, 4975−4977.
(32) Nishina, K., Unno, T., Uno, Y., Kubodera, T., Kanouchi, T., Mizusawa, H., and Yokota, T. (2008) Efficient in vivo delivery of siRNA to the liver by conjugation of α-tocopherol. *Mol. Ther. 16*, 734−740.
(33) Chiu, Y.-L., Ali, A., Chu, C.-Y., Cao, H., and Rana, T. M. (2004) Visualizing a correlation between siRNA localization, cellular uptake, and RNAi in living cells. *Chem. Biol. 11*, 1165−1175.
(34) Moschos, S. A. S., Jones, S. W. S., Perry, M. M. M., Williams, A. E. A., Erjefalt, J. S. J., Turner, J. J. J., Barnes, P. J. P., Sproat, B. S. B., Gait, M. J. M., and Lindsay, M. A. M. (2007) Lung delivery studies using siRNA conjugated to TAT(48-60) and penetratin reveal peptide induced reduction in gene expression and induction of innate immunity. *Bioconjugate Chem. 18*, 1450−1459.
(35) Muratovska, A., and Eccles, M. R. (2004) Conjugate for efficient delivery of short interfering RNA (siRNA) into mammalian cells. *FEBS Lett. 558*, 63−68.
(36) Gunasekaran, K., Nguyen, T. H., Maynard, H. D., Davis, T. P., and Bulmus, V. (2011) Conjugation of siRNA with comb-type PEG enhances serum stability and gene silencing efficiency. *Macromol. Rapid Commun. 32*, 654−659.
(37) Kim, S. H., Jeong, J. H., Lee, S. H., Kim, S. W., and Park, T. G. (2006) PEG conjugated VEGF siRNA for anti-angiogenic gene therapy. *J. Controlled Release 116*, 123−129.
(38) Rozema, D. B., Lewis, D. L., Wakefield, D. H., Wong, S. C., Klein, J. J., Roesch, P. L., Bertin, S. L., Reppen, T. W., Chu, Q., Blokhin, A. V., Hagstrom, J. E., and Wolff, J. A. (2007) Dynamic polyconjugates for targeted in vivo delivery of siRNA to hepatocytes. *Proc. Natl. Acad. Sci. U.S.A. 104*, 12982−12987.
(39) Lee, S. H., Mok, H., and Park, T. G. (2010) Di- and triblock siRNA-PEG copolymers: PEG density effect of polyelectrolyte complexes on cellular uptake and gene silencing efficiency. *Macromol. Biosci. 11*, 410−418.
(40) Choi, S. W., Lee, S. H., Mok, H., and Park, T. G. (2010) Multifunctional siRNA delivery system: polyelectrolyte complex micelles of six-arm PEG conjugate of siRNA and cell penetrating peptide with crosslinked fusogenic peptide. *Biotechnol. Prog. 26*, 57−63.
(41) Heredia, K. L., Nguyen, T. H., Chang, C.-W., Bulmus, V., Davis, T. P., and Maynard, H. D. (2008) Reversible siRNA-polymer conjugates by RAFT polymerization. *Chem. Commun. (Cambridge, U. K.)*, 3245−3247.
(42) Xu, J., Boyer, C., Bulmus, V., and Davis, T. P. (2009) Synthesis of dendritic carbohydrate end-functional polymers via RAFT: versatile multi-functional precursors for bioconjugations. *J. Polym. Sci., Part A: Polym. Chem. 47*, 4302−4313.
(43) Convertine, A. J., Benoit, D. S. W., Duvall, C. L., Hoffman, A. S., and Stayton, P. S. (2009) Development of a novel endosomolytic diblock copolymer for siRNA delivery. *J. Controlled Release 133*, 221−229.
(44) Convertine, A. J., Diab, C., Prieve, M., Paschal, A., Hoffman, A. S., Johnson, P. H., and Stayton, P. S. (2010) pH-Responsive Polymeric Micelle Carriers for siRNA Drugs. *Biomacromolecules 11*, 2904−2911.
(45) Benoit, D. S. W., Henry, S. M., Shubin, A. D., Hoffman, A. S., and Stayton, P. S. (2010) pH-responsive polymeric sirna carriers sensitize multidrug resistant ovarian cancer cells to doxorubicin via knockdown of polo-like kinase 1. *Mol. Pharmaceutics 7*, 442−455.
(46) Palanca-Wessels, M. C., Convertine, A. J., Cutler-Strom, R., Booth, G. C., Lee, F., Berguig, G. Y., Stayton, P. S., and Press, O. W. (2011) Anti-CD22 antibody targeting of pH-responsive micelles enhances small interfering RNA delivery and gene silencing in lymphoma cells. *Mol. Ther. 19*, 1529−1537.
(47) Crownover, E., Duvall, C. L., Convertine, A., Hoffman, A. S., and Stayton, P. S. (2011) RAFT-synthesized graft copolymers that enhance pH-dependent membrane destabilization and protein circulation times. *J. Controlled Release 155*, 167−174.
(48) Crownover, E. F., Convertine, A. J., and Stayton, P. S. (2011) pH-responsive polymer-antigen vaccine bioconjugates. *Polym. Chem. 2*, 1499−1504.
(49) Scales, C., Vasilieva, Y., Convertine, A., Lowe, A., and McCormick, C. (2005) Direct, controlled synthesis of the non-immunogenic, hydrophilic polymer, poly(*N*-(2-hydroxypropyl)-methacrylamide) via RAFT in aqueous media. *Biomacromolecules 6*, 1846−1850.
(50) Scales, C. W., Huang, F., Li, N., Vasilieva, Y. A., Ray, J., Convertine, A. J., and McCormick, C. L. (2006) Corona-stabilized interpolyelectrolyte complexes of SiRNA with nonimmunogenic, hydrophilic/cationic block copolymers prepared by aqueous RAFT polymerization. *Macromolecules 39*, 6871−6881.
(51) Xie, F., Woodle, M., and Lu, P. (2006) Harnessing in vivo siRNA delivery for drug discovery and therapeutic development. *Drug Discovery Today 11*, 67−73.
(52) Torchilin, V. (2005) Recent advances with liposomes as pharmaceutical carriers. *Nat. Rev Drug Discovery 4*, 145−160.
(53) Puri, A., Loomis, K., Smith, B., Lee, J.-H., Yavlovich, A., Heldman, E., and Blumenthal, R. (2009) Lipid-based nanoparticles as pharmaceutical drug carriers: from concepts to clinic. *Crit. Rev. Ther. Drug Carrier Syst. 26*, 523−580.